Characterization of Fungal Melanins from Black Stains on Paper Artefacts

Daniela Melo [1], Tiago G. Paiva [2] , João A. Lopes [3], Marta C. Corvo [2],* and Sílvia O. Sequeira [4],*

1   Department of Conservation and Restoration, NOVA School of Science and Technology,
     NOVA University Lisbon, 2829-516 Caparica, Portugal
2   i3N | Cenimat, Department of Materials Science (DCM), NOVA School of Science and Technology,
     NOVA University Lisbon, 2829-516 Caparica, Portugal
3   Research Institute for Medicines-iMed.ULisboa, Faculdade de Farmácia, Universidade de Lisboa,
     Av. Prof. Gama Pinto, 1649-003 Lisbon, Portugal
4   LAQV-REQUIMTE, Department of Conservation and Restoration, NOVA School of Science and Technology,
     NOVA University Lisbon, 2829-516 Caparica, Portugal
*   Correspondence: marta.corvo@fct.unl.pt (M.C.C.); silvia.sequeira@fct.unl.pt (S.O.S.)

Abstract: Melanins play a fundamental role in the biology and ecology of several fungal species. Unfortunately, this group of amorphous macromolecules also severely (and most times irreversibly) stains cultural heritage objects. Despite efforts made throughout the years, knowledge of the chemical composition and structure of melanins is still insufficient, which hampers the task of safely cleaning these colourants from cultural heritage materials in a targeted way without causing further deterioration. This work aimed therefore to contribute towards enlightening the characteristics of fungal melanins from three fungi that are common paper colonizers: *Aspergillus niger*, *Chaetomium globosum* and *Cladosporium cladosporioides*. The extracted melanins were characterized by FTIR, Raman, UV-vis, Solid-State NMR and MALDI-TOF MS spectroscopies and the effect of inhibitors of DHN-melanin and DOPA-melanin pathways on colony pigmentation and growth was evaluated. Although all the extracted colourants show a predominantly aromatic structure with carbonyl and phenolic groups, some differences between the melanins can be highlighted. Melanins obtained from *Ch. globosum* and *Cl. cladosporioides* exhibited similar structures and composition and both presented DHN-melanin characteristics, while *A. niger*'s melanins revealed a more complex and ordered structure, with a higher prevalence of highly conjugated carbonyls than the others, besides the additional presence of a yellow/green component. These conclusions cannot be overlooked while selecting targeted cleaning methodologies for melanin stains on cultural heritage materials.

Keywords: melanin; filamentous fungi; *Aspergillus niger*; Solid-State NMR; MALDI-TOF MS

1. Introduction

Filamentous fungi are one of the main etiological agents of deterioration on our cultural heritage. Artworks and documents made of paper are particularly susceptible to fungal colonization due to the organic composition and hygroscopicity of this material [1]. Besides inducing chemical and physical decomposition, metabolic substances excreted by fungi, and fungal cells themselves, are often pigmented, interfering with the readability and fruition of artefacts, diminishing their artistic, informative, and monetary value. Fungal stains on paper objects present a great variety of colours from black to brown, red, yellow, or purple, and can ultimately deem the objects unreadable [2,3]. Not surprisingly, fungal stain removal is considered one of the major topics needing further research in the field of paper biodeterioration [4].

Melanins, which are responsible for most brown and black fungal stains, are the utmost problematic colourants for paper documents and artworks, not only due to their frequent occurrence and visual impact, but also because they are the most permanent colourants and the hardest ones to safely remove from the paper matrix [5]. Besides their general insolubility on a wide range of polar and organic solvents and chemical recalcitrance, melanins show a high molecular heterogeneity and variability among different melanin-producing fungi [6]. To develop safer cleaning methodologies [7], a deeper knowledge of melanins' chemical structure and composition is therefore paramount, as highlighted by a recent review on fungal melanins affecting paper-based cultural heritage [6].

Melanin is not a single colourant, but rather a broad term for a group of natural colourants composed of amorphous polymeric molecules produced by most organisms. This group of colourants plays a fundamental role in the biology and ecology of several fungal species, conferring them survival advantages through protection against ultraviolet radiation or desiccation [6]. Recent research has also shown the role of melanins on fungal toxicity and resistance to disinfectants [8,9].

While some fungal species are constitutively melanised, others melanise only in specific developmental phases (e.g., conidia formation), under particular environmental conditions, or in the presence of phenolic melanin precursors [10]. Melanins are formed by oxidative polymerization of phenolic or indolic precursors, in a process that can involve multiple enzymes, or occur by spontaneous polymerisation [10]. The two most common types of fungal melanins are DHN-melanin (named after one of the pathway intermediates, 1,8-dihydroxynaphthalene–1,8-DHN) and DOPA-melanin (named after one of the precursors, L-3,4- dihydroxyphenylalanine) [11]. Although the structure of some polymer subunits has been discovered, a complete and detailed molecular structure of melanins is still to be determined [12]. These polymers feature extreme molecular heterogeneity, amorphous particulate character, and a lack of successful solvents, which have throughout the years, impaired an in-depth examination [13].

To contribute to the enlightenment on the chemical structure of fungal melanins responsible for staining paper documents and artworks, we selected three melanized fungi –which are among the most common paper colonizers–for melanin extraction and characterization: *Aspergillus niger* (*A. niger*), *Chaetomium globosum* (*Ch. globosum*) and *Cladosporium cladosporioides* (*Cl. cladosporioides*) [5,14]. FTIR, Raman, UV-vis, Solid-State NMR and MALDI-TOF MS spectroscopic techniques aided the chemical characterization of the extracted melanins. The selected fungi were also cultured with different inhibitors of melanin precursors, towards understanding which are the melanin biosynthetic pathways.

The purpose of this work was therefore to identify the differences and similarities in the melanin structures of different fungi, providing a rationale for the future development of targeted cleaning methodologies.

2. Materials and Methods

2.1. Fungal Cultures

A. niger van Tieghem, *Ch. globosum* Kunze and *Cl. cladosporioides* (Fresen.) G.A. de Vries were isolated from fungal stains on paper documents and identified by DNA analysis at Universidade de Coimbra (Coimbra, Portugal) [15,16]. *A. niger* and *Cl. cladosporioides* were grown in liquid malt extract broth (MEB). *Ch. globosum* was grown in malt extract agar (MEA) since the solid medium favoured the formation of reproductive structures where melanin is located (ascomata and ascospores). Incubation was performed for 30 days at 25 °C in the dark. All fungal cultures were prepared in triplicate.

2.2. Extraction and Purification of Melanins

The extraction and purification processes were adapted from the literature [17]. After incubation, fungal biomasses were collected by vacuum filtration. Solid MEA from *Ch. globosum* culture had to be liquefied by boiling in distilled water previously to filtration. The obtained individual fungal biomasses were separately crushed with 2 M NaOH in a mortar and allowed to stand for 48 h. After a second filtration to remove fungal debris, the resulting filtrates were acidified with 2 M HCl and allowed to precipitate overnight. The precipitates were collected after centrifugation at 180 rpm for 10 min and further purified by acid hydrolysis using 6 M HCl at 100 °C for 2 h, to remove carbohydrates and proteins. After collection by centrifugation, precipitates were treated with organic solvents: chloroform, ethyl acetate and ethanol, to remove lipids. The resulting compounds were dried at room temperature, dissolved in 2 M NaOH and vacuum filtered. The collected filtrates were precipitated with 6 M HCl (kept overnight), washed with distilled water and allowed to dry at room temperature. These precipitates were considered to be purified melanin and were used for further analyses. All extracted and purified melanin samples were compared to synthetic melanin (DOPA-melanin, Sigma-Aldrich). A chitin sample (chitin from shrimp shells, practical grade, Sigma-Aldrich, Saint Louis, MI, USA), was also analysed as a reference for the FTIR spectroscopy.

2.3. Inhibition of Melanin Formation by Pathway-Specific Inhibitors

To differentiate melanin biosynthesis pathways in the studied fungal species, the effect of inhibitors of DHN-melanin pathway (tricyclazole) and DOPA-melanin pathway (kojic acid) on colony pigmentation and growth was evaluated. Tricyclazole (Dr Ehrenstorfer GmbH, Augsburg, Germany), or kojic acid (Alfa Aesar, MA, USA), both dissolved in ethanol, were added to autoclaved and cooled PDA medium to give a final concentration of 100 μg·m^{-1} [11] and plated in 60 mm Petri dishes. Control plates consisted of PDA mixed with ethanol at the same proportion used in plates with inhibitors (1% *v/v*). All assay variants were prepared in triplicate. PDA plates were inoculated with a mycelium plug of 3 mm diameter cut from the margins of an actively growing colony and incubated for 10 days at 25 °C in the dark. Fungal growth was evaluated by colony area measurements, as described in a previous publication [18].

2.4. μ-FTIR Analysis

Micro Fourier transform infrared spectroscopy (μ-FTIR) was performed on a Nicolet Nexus spectrophotometer interfaced with a Continuμm microscope and an MCT-A detector cooled by liquid nitrogen. The spectra were collected in transmission mode, with a 50–100 μm spatial resolution, 4 cm^{-1} optical resolution and 128 co-added scans, using a thermo-diamond anvil compression cell.

2.5. UV-Vis Analysis

Melanin samples were dissolved in 0.1 M NaOH and their absorption spectra were recorded using quartz cells, in the wavelength range of 200–600 nm, on a T90+ UV-visible spectrometer (PG Instruments, Leicestershire, UK).

2.6. μ-Raman Analysis

Raman microscopy was performed in a Labram 300 Jobin Yvon spectrometer, using a solid-state laser operating at 532 nm. Spectra were recorded as an extended scan. The laser beam was focused either with a 50× or a 100× Olympus objective lens. The laser power at the surface of the melanin samples was varied with the aid of a set of neutral density filters (optical densities 0.6, 1 and 2), with laser power intensities varying between 2.5 and 0.1 mW.

2.7. Solid-State (SS) NMR Analysis

^{13}C CP/MAS spectra were obtained on an Avance III WB spectrometer operating at 7.2 T, corresponding to a 300 MHz Larmor frequency for ^{1}H and 75 MHz for ^{13}C. Melanin samples were packed into 4 mm zirconium rotors and sealed with Kel-F caps. In selected experiments, an insert was packed with the sample and placed inside the rotor. The samples were spun at the magic angle at 5–10 kHz. Cross-polarization was performed by applying a variable spin-lock sequence RAMP-CP/MAS with a contact time of 1.2 s and a recycle delay of 2 s. A total of 5000 points were sampled and accumulated during 4000–15,000 transients. Chemical shifts are reported in ppm.

2.8. Mass Spectral Analysis

MALDI MS spectra were acquired using a ULTRAFEX III TOF/TOF (Bruker) mass spectrometer equipped with a smartbeam laser. All spectra were acquired in the positive linear mode in a 1–20 KDa mass range. The matrix used for analysis was composed of 2,5-dihydroxybenzoic acid (DHB) dissolved in TA30, at a 20 mg·mL^{-1} concentration. The analysed melanin samples were prepared by dilution in two different solvents, NH$_4$OH 25% or ACN-TFA 4%. For the preparation of the MALDI plate, 1 µL of each melanin sample mixed with the DHB matrix (50:50 *v/v*) was applied to the plate and left to dry at room temperature. Fungal melanins were initially analysed by MALDI-TOF using ACN-TFA 4% as a solvent, as described by Beltrán-García and colleagues [19]. However, in the present study, melanin samples precipitated with ACN-TFA, and NH$_4$OH 25% were used instead to improve solubilization.

The identification of a repeating peak pattern in MS signals, characteristic of the presence of polymers, was performed according to the combination of two strategies: Fourier-transform and difference vector calculation. The MS signal was first processed by normalizing for the maximum peak intensity, followed by the application of a peak identification algorithm (Vectorized Peak Detection) [20]. Relative intensities corresponding to detected peaks were preserved and all remaining intensities were set to zero. The processed signal was then analysed with Fourier transform (FT) to convert the *m/z* domain signal to a frequency domain signal, highlighting in this way repeating *m/z* patterns characteristic for example of fragments originating from polymers. The FT result was filtered and the frequency signals above a specific threshold (hereby defined as 10% of the maximum frequency domain signal) were cancelled. The application of the inverse FT produced a filtered signal [21], from which a simple vector difference (subtraction of every consecutive intensity) was calculated. The histogram of the difference vector highlighted the *m/z* (s) of repeating peaks. Because there might be different size fragments, single histogram peaks were not expected (whilst in some situations a single peak was found). To effectively estimate the *m/z* of the polymer-originated fragments the peaks in each histogram were combined with the FT frequencies generating the *m/z* undoubtedly corresponding to repeating patterns. The algorithm was produced in Matlab version 2019b (Mathworks, Natick, MA, USA) and applied to every MS signal. A comparison was then made between the samples.

3. Results

3.1. Melanin Synthesis Pathway

Colonies of *Ch. globosum* and *Cl. cladosporioides* became paler when grown with the DHN-melanin pathway inhibitor (tricyclazole), while no pigmentation difference is observed regarding the DOPA-melanin inhibitor (Figure 1). Tricyclazole not only inhibited melanin production in *Ch. globosum*, but also significantly hindered its growth (Supplementary Figure S1). On *Cl. cladosporioides*, this inhibitor caused a shift in the colonies' colour to a brownish/orange hue (Figure 1), also observed by Llorente and colleagues [22].

A. niger's colonies became denser when grown with tricyclazole (Figure 1), exhibiting olive green conidia at 10 days of incubation. Nevertheless, the colour difference regarding the controls was not obvious as with the other two fungi. The size of the colonies obtained with both melanin inhibitors was also not significantly different from the controls (Supplementary Figure S1). In Supplementary Figure S2 we can observe all replicate plates for *A. niger*, which corroborate this uncertainty regarding the inhibitory effect of tricyclazole.

Interestingly, the presence of kojic acid (DOPA-melanin inhibitor) seems to have stimulated the production of melanised conidia in *A. niger*'s colonies, which were denser and darker than in the control sample (Figure 1).
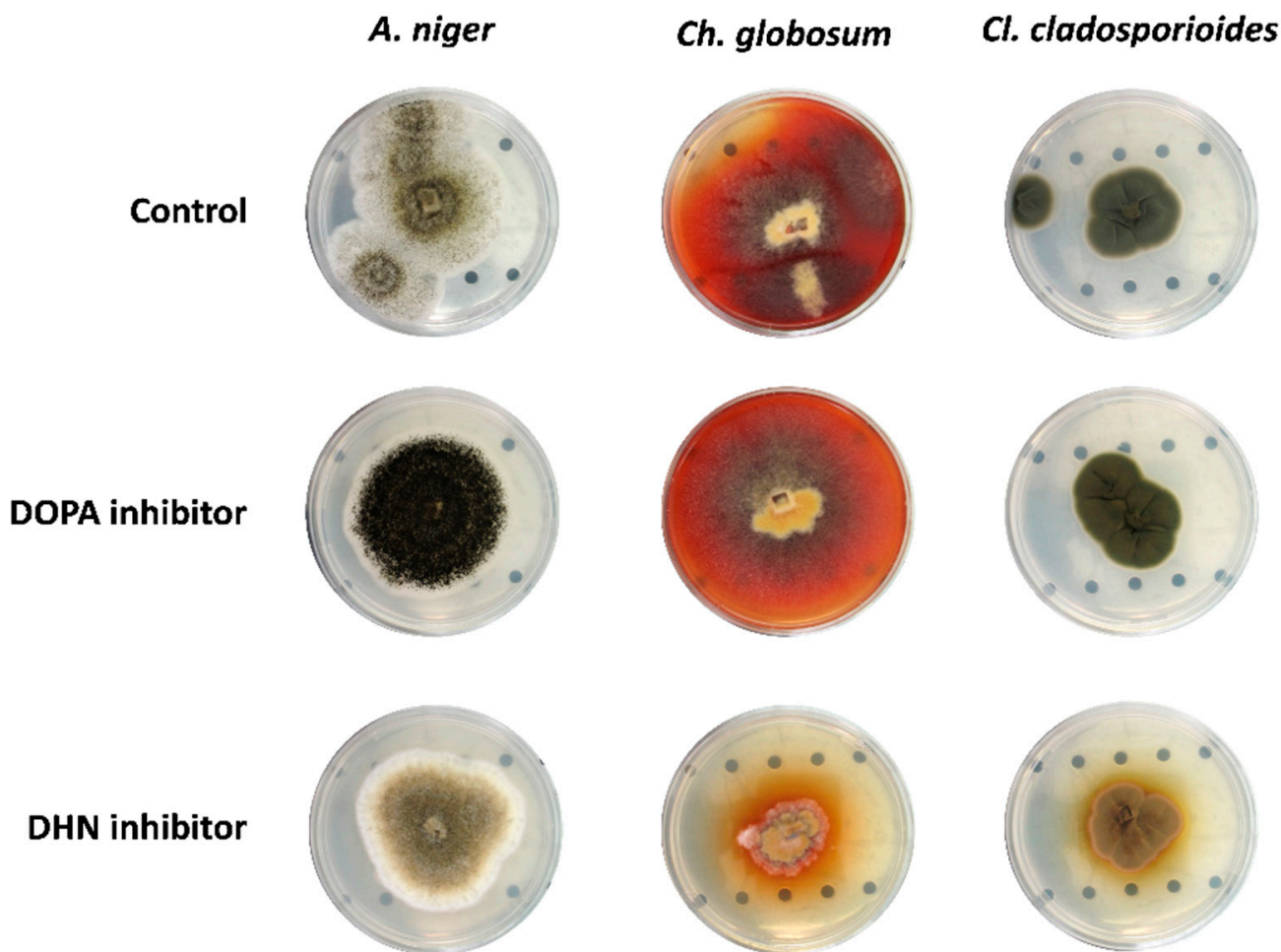
Figure 1. Colonies of *A. niger*, *Ch. globosum* and *Cl. cladosporioides* grown on PDA in the absence (Control) and presence of kojic acid (DOPA inhibitor) or tricyclazole (DHN inhibitor), at 10 days of incubation (25 °C in the dark).
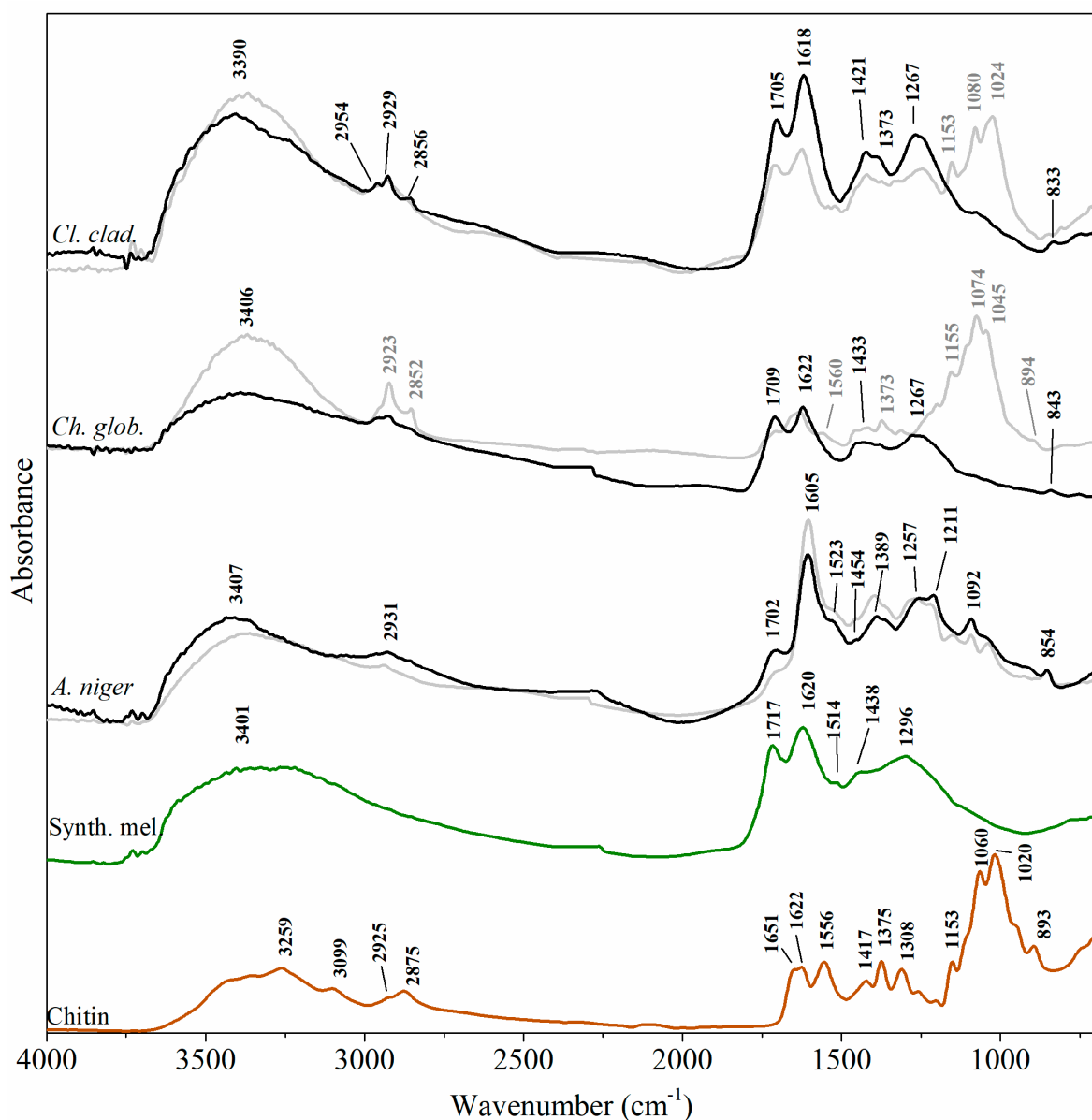
3.2. μ-FTIR Analysis

FTIR spectra of fungal melanins after extraction (Figure 2—light-grey lines) and after purification (Figure 2—black lines) illustrate the relative efficacy of both processes.

Spectra of fungal extracts, particularly the ones from *Ch. globosum* and *Cl. Cladosporioides*, still exhibit characteristic bands of chitin (bottom spectrum in Figure 2): 2924–2929 and 2854 cm^{-1} (νCH); 1650–1620 cm^{-1} (Amide I: νC=O); ~1560 cm^{-1} (Amide II: ν N-H); 1424 and 1370 cm^{-1} (CHx deformations in β-chitin); 1075 cm−1 (νC-O); and 1022–1041 cm^{-1} (νC-O-C in β-chitin) [23–25]. This illustrates that an extraction procedure alone was not sufficient for the isolation of melanin. On the purified fungal pigment's spectra (Figure 2—black lines) chitin bands are much less intense or even absent, and characteristic bands of melanins (Table 1) are evidenced.

Spectra obtained before and after purification of *A. niger*'s melanin are nearly coincidental (Figure 2). Bands attributed to cell wall carbohydrates were much less intense than on the other two fungi, showing that for this species, melanin was already quite pure before the purification step. Purified *A. niger*'s spectra slightly differ from the ones of the other two fungi, namely on a more intense peak at 1605 cm^{-1}, slightly dislocated to lower wavenumbers, and a much less intense 1702 cm^{-1} peak, which indicates a predominance of conjugated carbonyls over unconjugated ones on this sample.

Also, a peak at 1523 cm^{-1}, attributed to the bending vibration of N-H and stretching vibration of C-N (secondary amine) [26] can be found for *A. niger*. This band can be assigned to residues of proteins or chitin (chitin reference and unpurified *Ch. globosum* show peaks at 1556–1560 cm^{-1}) on the sample. Nevertheless, the synthetic melanin reference from Sigma (DOPA-melanin) also exhibits a peak at 1514 cm^{-1}, which is attributed to the presence of indole groups in DOPA-melanins [27].

Figure 2. µFTIR spectra obtained from a chitin reference, synthetic melanin, and melanin extracts from *A. niger*, *Ch. globosum* and *Cl. Cladosporioides*, before (light-grey lines) and after purification (black lines).

3.3. UV-Vis Analysis

Purified fungal melanins and reference synthetic melanin show broad, strong absorbance in the UV region, with maxima at ~220 nm (Figure 3). While this type of absorption is atypical in organic chromophores, it is a characteristic of melanin pigments [31], and probably results from the considerable structural heterogeneity and disorder of these colourants. This leads to an overlapping of energy levels, with a greater number of electronic transitions along the electromagnetic spectrum and, consequently, an extension of the absorption spectrum.

Table 1. Assignment of the main absorbance bands in the infrared spectra (μ-FTIR) obtained from purified fungal extracts and synthetic melanin.

|		Wavenumber (cm^{-1})		Assignment	References
Synth.	A. niger	Ch. globosum	Cl. cladosporioides		
3401	3407	3406	3390	νO-H; νN-H	[27–29]
	2931	2923	2954; 2929; 2856	Aliphatic νC-H2 and νC-H3; νN-H	[27,29,30]
1717	1702	1709	1705	ν C=O unconjugated with benzene ring	[28]
1620	1605	1622	1618	νC=O; νC=C aromatic (from conjugated quinone structures)	[22,28,30]
1514	1523			δN-H; νC-N	[22,28–30]
1438	1454; 1389	1421	1432	νC-N; δC-H3 and δC-H2)	[22,27–30]
1296	1257	1267	1267	νC-OH (alcoholic, carboxylic, phenolic groups);	[22,27,28,30]
	1092	1080		Alcoholic C-O; C-H in-plane of aliphatic structure	[22,27–29]
	854	843	833	δC-H out-of-plane in aromatic structure	[27,29]

ν—stretching; δ—bending.
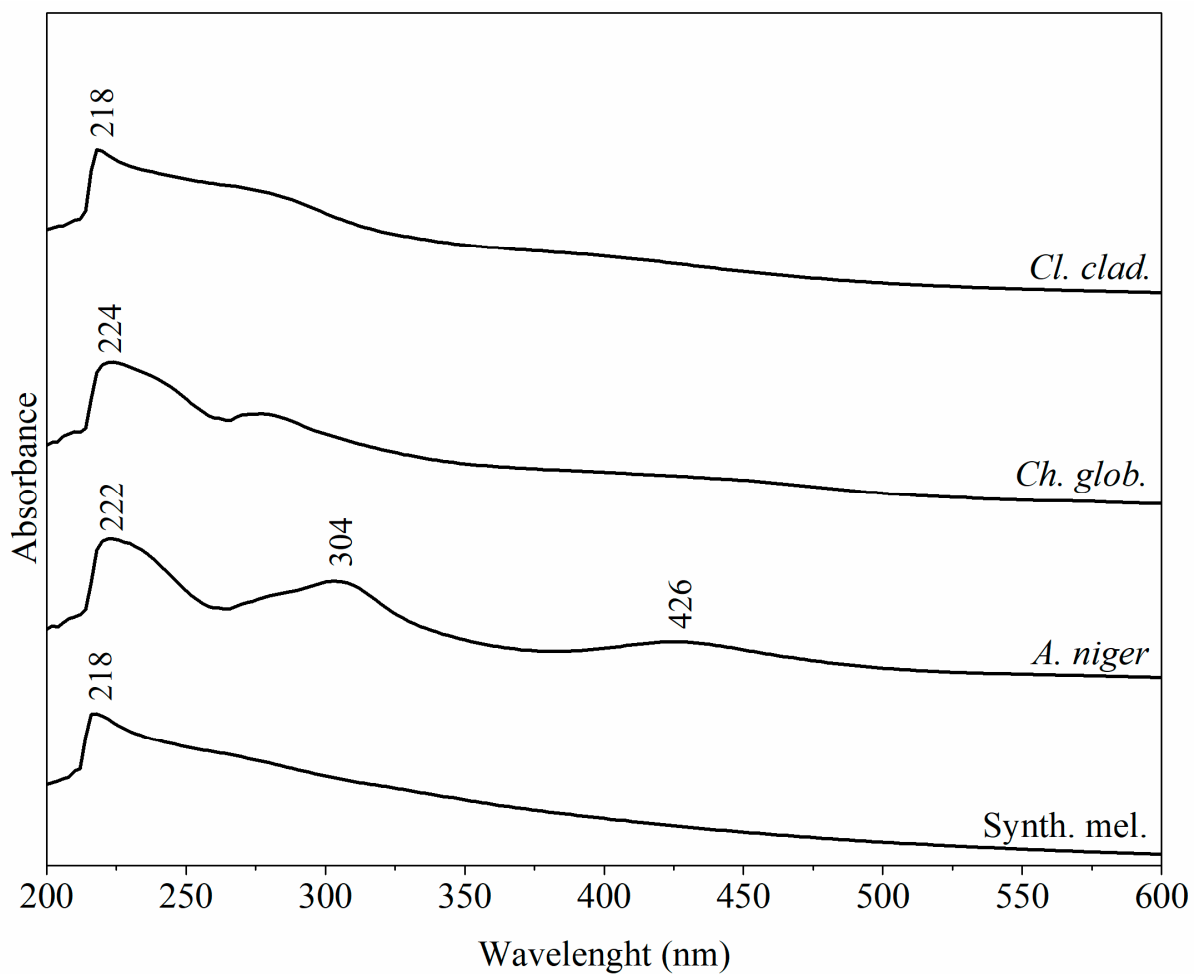
Figure 3. UV-vis spectra of purified fungal melanins and synthetic melanin.

A. niger's spectrum additionally shows two weaker broad bands, one centred at 304 nm (UV region) and another at 426 nm (visible region of the electromagnetic spectrum). These bands can be ascribed to the presence of conjugated systems, such as naphtho-γ-pyrones [32]. However, another possible explanation, especially regarding the 426 nm band, emitting in the yellow-green region, could be the presence of a green pigment (a hexahydroxyl pentacyclic quinoid) that is linked to melanin in *A. niger*'s aspergillin [33,34].

3.4. μ-Raman Analysis

The obtained Raman spectra are dominated by two broad bands: a higher intensity band with maxima between 1567–1621 cm^{-1} and a second band located between 1340–1387 cm^{-1} (Figure 4), both characteristics of general melanin Raman spectra [35–37]. A broadband background is noticeable due to the autofluorescence emission properties of melanin. Huang et al. [37], using multiple wavelengths and a variety of melanin sources, have shown that the two prominent peaks observed in melanins are indeed due to inelastic Raman scattering rather than fluorescence or other nonlinear processes.
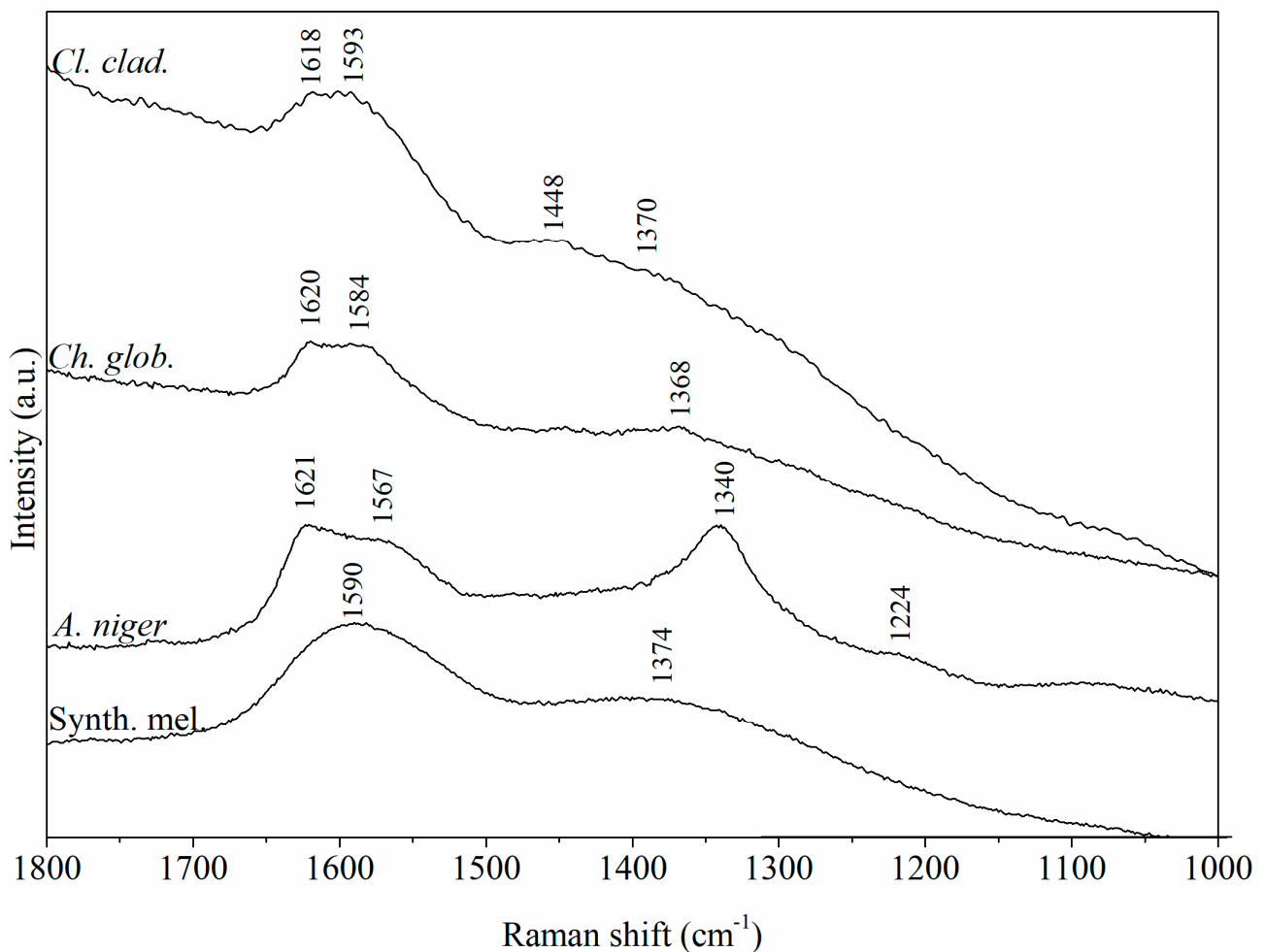
Figure 4. μ-Raman spectra from synthetic reference and purified melanins.

While on the synthetic melanin reference we observe a single band centred at 1590 cm^{-1}, on fungal extracts we see two distinct and partially overlapped bands: one at 1597–1593 cm^{-1}, and another at 1618–1621 cm^{-1}. This overlapping has already been observed before on Raman spectra obtained from black fungi [38]. The broad features of these spectra are probably due to the conjunction of many overlapping Raman bands owed to the vibrations of the various constituent monomers [36].

These two bands have been assigned to C=C stretching vibrations and aromatic ring stretch, respectively, in polycyclic aromatic compounds [38,39].

Cl. cladosporioides exhibits a weak band at 1448 cm^{-1}, attributed to C–H deformations in aliphatic chains, proteins or polysaccharides, probably derived from cell wall residues [36,38].

A. niger's sample shows higher intensity on the 1340–1387 cm^{-1} band, which has been attributed to C-O stretching vibrations and C–H vibrations in methyl and methylene groups in polyphenols [38,39]. The weak band at 1224 cm^{-1} in *A. niger*'s spectrum can be attributed to C–O stretching/OH in-plane deformation in COOH [35].

3.5. Solid-State (SS) NMR Analysis

^{13}C CP/MAS spectra of the melanin samples revealed differences in chemical shift regions, intensities of bands and linewidth of peaks (Figure 5). Table 2 presents the characteristic chemical shift regions for the obtained spectra.
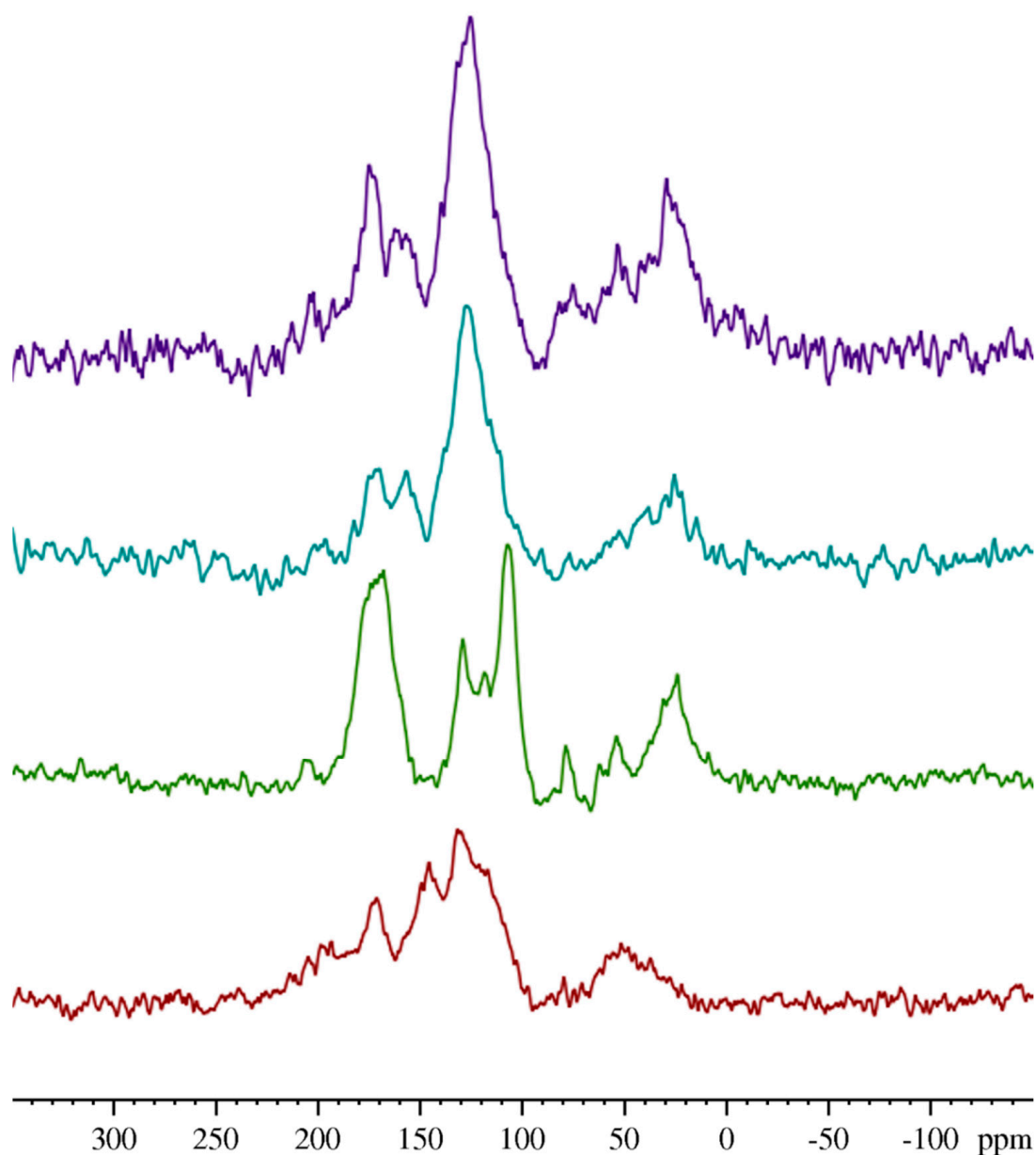
Figure 5. ^{13}C CP/MAS spectra of synthetic melanin (red) and melanins produced by *A. niger* (green), *Ch. globosum* (blue) and *Cl. cladosporioides* (purple).

Table 2. Characteristic chemical shift regions in ^{13}C CP/MAS Spectra.

Melanin	Carbonyl	Aromatic		Aliphatic
		Cq	CH	
A. niger	188–153 (Carbonyl + Cq)		135–100	80–10
Cl. cladosporioides	180–165	165–150	145–95	66–10
Ch. globosum	180–165	160–147	145–95	50–10
Synthetic	180–160	157–142	140–100	67–30

Note: CH represents protonated carbons and Cq represents non-protonated carbons.

According to our results, the analysed samples are predominantly aromatic with phenol groups, having some fragments oxidized to carbonyls, which is consistent with the type of structures expected for fungal melanins and the results obtained above, which also revealed the presence of carbonyl, phenolic and aromatic groups.

The synthetic melanin used in this study was obtained from the oxidation of L-Tyrosine with H_2O_2 in DMSO [40]. The broad and poorly resolved ^{13}C CP/MAS signals here obtained are an indication of a heterogeneous sample, a disordered amorphous material with a high molecular weight (MW). These ^{13}C chemical shifts are compatible with the presence of tyrosine-derived compounds similar to the ones found in the literature (Table S1) [41,42]. However, none of the analysed fungal melanins demonstrated a similar profile.

Both *Cl. cladosporioides* and *Ch. globosum* melanins present similar ^{13}C CP/MAS spectra (Figure 5, Table 2), exhibiting a broad peak width, also indicating higher MW polymers. These spectra are compatible with melanins from the 1,8-DHN pathway, which is following the results obtained in Section 3.1 and the literature [22,43]. Comparing the observed ^{13}C chemical shifts with the ones from model compounds in literature (Table S1) [44–48], these are in better agreement with the naphthalene phenol groups resonating at 160 ppm, than with L-DOPA derivatives, as the L-DOPA catechol ring resonates closer to 140 ppm, which is closer to the chemical shift found in synthetic melanin for quaternary carbons.

Within all melanin samples, the one produced by *A. niger* is considerably different from the rest. Its ^{13}C CP/MAS spectrum (Figure 5, Table 2) exhibits sharper peaks, a possible indication of a more organized sample, and/or lower MW. Regarding characteristic regions, aromatic and carbonyl chemical shifts are different in *A. niger*'s spectrum, with a notorious predominance of carbonyls, contrary to the rest. This behaviour can be attributed to the higher oxidation of its monomers [49], which amounts to more intense signals in the carbonyl region. Moreover, structures with highly conjugated carbonyls, as observed in the µFTIR spectra, are also compatible with the observed NMR spectra. Another feature that stands out, is the presence of a sharp peak resonating at 107 ppm, which possibly indicates the presence of conjugated cyclic ketones moieties.

All analysed fungal melanins exhibit aliphatic carbon resonances between 80 and 10 ppm, which can be explained by either the presence of saturated carbons from the DHN biosynthetic pathway or the presence of chitin moieties covalently bonded to melanin.

Comparing carbonyl regions of all fungal melanins (Figure 5, Table 2), *Cl. cladosporioides* and *Ch. globosum*, exhibit a narrower chemical shift interval (180–165 ppm), more compatible with the presence of ketones, carboxylic esters, or acids, while *A. niger* presents a broader interval (188–153 ppm) that can include the presence of amide carbonyls.

The MW difference between natural and synthetic melanin is conflicting within the literature, which reports either similar MW regardless of the source, or a higher size in naturally produced melanins [50]. In our study, the different behaviour of *A. niger*'s melanin may be ascribed to the presence of a lower MW polymer, possibly a hybrid structure, due to the presence of different types of monomers, but with a more ordered overall pattern.

Without further analysis, it is only possible to ascertain that, regarding the observed differences between the carbonyl and aromatic regions of the obtained spectra, melanins produced by *Ch. globosum* and *Cl. cladosporioides* are clearly from the same biosynthetic pathway, while *A. niger*'s melanin does not peacefully fit this classification.

3.6. Mass Spectral Analysis

To further rationalize fungal melanin's structure, we performed mass spectrometry in our samples, initially using ACN-TFA 4% as solvent. These conditions were described by Beltrán-García and colleagues, which obtained a MALDI-TOF spectrum of fungal melanin with constant and well-defined spacings of 161.8 Da between peaks, attributing it to 1,8-DHN (MW = 160.17) [19]. However, in the present study, melanin precipitated in ACN-TFA (acidic solvent) and the obtained spectra revealed characteristic peaks of chitin decomposition (results not shown), which are also compatible with the *m/z* obtained by Beltrán-García et al. [19,51]. To improve sample solubilization, we used NH4OH 25% instead, and MALDI-TOF spectra were successfully obtained (supplementary Figures S3–S6). The acquired mass spectra are not characteristic of regular homopolymers, which is in accordance with previous work [52]. The search for a fragmentation pattern in these complex MALDI-TOF spectra lead us to develop and apply an algorithm to analyse the repeating peak patterns in MS spectra, searching for the relative intensities corresponding to detected peaks (Supplementary Figure S7).

Synthetic melanin did not reveal an *m/z* fragmentation pattern identifiable with possible melanin monomers (Supplementary Figure S7). In this case, the synthetic polymerization procedure with H_2O_2 oxidation may lead to a more random structure, where the *m/z* 19 fragmentation pattern most probably corresponds to water molecules being released. We observe this same *m/z* 19 fragmentation in *A. niger* and *Cl. cladosporioides*' samples.

Melanins from *Ch. globosum* and *Cl. cladosporioides* exhibit similar fragmentation patterns, confirming our previous findings regarding their structural resemblance, while *A. niger* once more diverged from these two and also from the synthetic melanin (Supplementary Figure S7).

4. Discussion

The nature of purified colourants obtained from *A. niger*, *Ch. globosum* and *Cl. cladosporioides* was confirmed by their spectral profiles along all the analyses performed, demonstrating the presence of melanins. Melanins obtained from *Ch. globosum* and *Cl. cladosporioides* showed similar characteristics among each other, while *A. niger*'s colourants, on the other hand, stood out from the rest, exhibiting distinct characteristics from all the analysed melanins, including the synthetic sample.

Our analyses, and especially FTIR, evidenced the need for a purification step to remove cell wall carbohydrates from the extracted fungal pigments, especially for *Ch. globosum* and *Cl. cladosporioides*. Fungal melanins may be secreted into the environment or located in the cell wall where they are most likely cross-linked to cell wall polysaccharides (glucan and chitin) [12,19,53]. Depending on the fungal species, melanin can be found either on the inner or the outer layers of the cell wall. While the inner layer is made mainly of beta-glucans, chitin and small amounts of proteins, the outer layers contain high levels of mannoproteins [53]. On *A. niger*'s spectra, bands attributed to cell wall carbohydrates were not so evident in the non-purified sample, which could indicate that in this species, melanins are synthesised in the outer layers of cell walls or have a lower degree of crosslinking with cell wall polysaccharides [12].

Regarding the colour of our melanin samples, we can see in the obtained UV-vis spectra that there is absorption throughout the entire visible region. Among biological colourants, only melanins have this type of absorption. Since the colours we observe result from a selective light absorption process, if all wavelengths of light are absorbed and none reflected, we recognize it as black. The aromaticity of the units that make up the melanin structure favours efficient electronic delocalization, which contributes to the stabilization of the polymer and, consequently, to an increase in its photo-protective capacity [54]. This is in agreement with the suggested photoprotection function of melanins [31]. We could also observe evidence of a yellow-green compound in the UV-vis spectrum of *A. niger*'s sample, through the band at 426 nm (emission in the yellow-green region). This colourant could contribute to the olive-green colouration observed in *A. niger*'s colonies treated with tricyclazole (Figure 1).

The results obtained with melanin pathway inhibitors indicate that both *Cl. cladosporioides* and *Ch. globosum* produce melanin via the DHN biosynthetic pathway, which is in line with previous studies [22,43]. Nevertheless, the significance of DHN- and DOPA-melanin pathways in the biosynthesis of *A. niger*'s melanin is still unclear and controversial [55]. Pigmentation in this species has shown to be resistant to the DHN pathway inhibitor tricyclazole [17,56]. Also, according to Jørgensen et al., homologous genes of central DHN-melanin pathway genes are missing in *A. niger* [33]. Pal and colleagues claimed that *A. niger* produced melanin via the DOPA pathway, after obtaining a total inhibition of melanisation with kojic acid, a DOPA inhibitor [17]. However, they lacked an investigation of solvent controls, and the observed inhibitory effect on *A. niger* was later confirmed to be caused by the dimethylsulfoxide (DMSO) used to dissolve kojic acid [11,57]. The research already gathered around *A. niger*'s conidial pigmentation reveals that it is more complex than previously thought [33,55] and further research is still needed.

A. niger's pigment sample revealed a much higher predominance of conjugated carbonyls over unconjugated ones when compared to the other two fungi. Ray and Eakin [34] proposed that aspergillin, the pigment responsible for the black colour in *A. niger*'s conidia, is formed from two precursor molecules—a low-molecular-weight (~368 Da) green pigment (identified as a hexahydroxyl pentacyclic quinoid); and a brown low-molecular-weight (~5000 Da) melanin pigment. The presence of this green pigment (also observed in our UV-vis spectrum) linked to melanin, which, according to Ray and Eakin [34] exhibits a strong infrared band at 1625 cm^{-1}, may be the reason for the relatively higher presence of conjugated carbonyls in *A. niger*'s pigment sample.

Comparing all the melanin's FTIR analyses, the presence of an amide functionality is also more probable in *A. niger*'s melanin. We could identify peaks that are characteristic of the bending vibration of N-H and the stretching vibration of C-N (secondary amine).

On the NMR spectra, *A. niger* also exhibits chemical shifts that indicate the presence of amide carbonyls. Several amides have already been identified as secondary metabolites in *A. niger* [58]. Ray and Eakin [34] analysed the nitrogen content of the two aspergillin precursors and concluded that the green pigment was nitrogen-free, while the melanin precursor was not.

Our mathematical approach to identifying repeating peak patterns in MALDI-TOF MS signals was vital to the interpretation of the acquired mass spectra, which, as expected, were not characteristic of regular homopolymers and presented a high complexity. Considering the *m/z* fragmentation patterns obtained from *Ch. globosum* and *Cl. cladosporioides* melanins (Figure S7), the *m/z* peaks at 338 intervals are a possible indication of a 1,8-DHN monomer (Figure 6a), and the *m/z* peak at 162 may illustrate the presence of another lower mass 1,8-DHN monomer (Figure 6b), or the presence of glucosamine units from chitin (Figure 6c) [51] derived from cell wall residues.
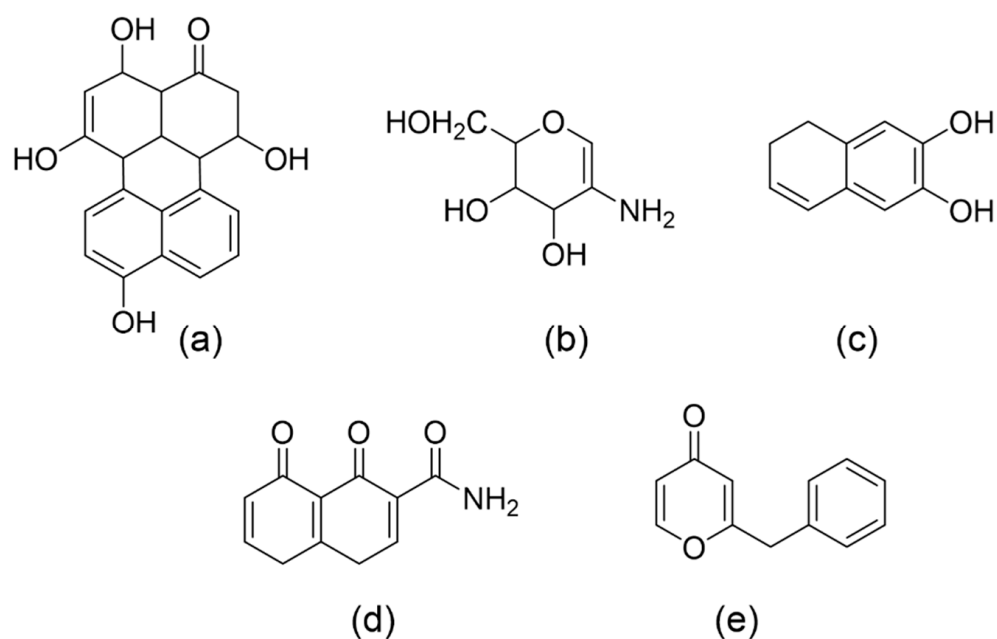
Figure 6. Possible structures present in pigment samples extracted from *Cl. cladosporioides* and *Ch. globosum* (**a–c**), and *A. niger* (**d,e**).

A. niger's melanin, however, does not produce a pattern identifiable with the same 1,8-DHN monomer, revealing instead the possible presence of a hybrid structure that can be traced back to *A. niger*'s secondary metabolites. This fungus is known to be a prolific source of functional biomolecules [58]. Accordingly, the *m/z* 203 fragmentation is compatible with the carboxamide shown in Figure 6d, a highly conjugated 1,8-DHN derived monomer with an amide function, which justifies both the NMR and FTIR results. Several amides have already been identified as secondary metabolites in *A. niger* [58]. Another frequent *A. niger* fragmentation is *m/z* 186, which may indicate the presence of nigerpyrone (Figure 6e), an *A. niger*'s secondary metabolite [59]. We cannot help to notice the resemblance between nigerpyrone and kojic acid (the DOPA-melanin inhibitor we used), which could shed some light on the results obtained with *A. niger* in Section 3.1, where a higher production of pigmented conidia was obtained in colonies grown with kojic acid.

5. Conclusions

Melanins produced by *Ch. globosum* and *Cl. cladosporioides* showed high similarity between them, in terms of structure and chemical composition, and are compatible with melanins from the 1,8-DHN biosynthetic pathway.

The melanin complex extracted from *A. niger* had a higher prevalence of highly conjugated carbonyls and either a more organized structure or lower MW than the others. Our results point out a possibly hybrid structure due to the presence of different types of monomers, but with a more ordered overall pattern, possibly with a higher degree of crystallinity. The presence of an amide functionality is also more probable in this melanin. We could also distinguish the presence of a secondary component emitting in the yellow-green region of the visible spectrum in *A. niger*'s samples, which could be attributed to a hexahydroxyl pentacyclic quinoid.

From the conservation of cultural heritage point of view, these results show that, contrary to the general idea in the field that all fungal melanins are similar, these macromolecules may exhibit different chemical profiles, different molecular weights, crystallinity levels, and additional pigments, which will most probably impact on the ease of their removal from affected artefacts. It is now important to study how the chemical properties of different melanins will impact the selection of different stain cleaning methodologies and aid the development of new, more targeted cleaning treatments to improve efficacy and prevent side effects.

Supplementary Materials: The following supporting information can be downloaded at: https://www.mdpi.com/xxx/s1, Figure S1: Measurement of *A. niger*, *Ch. globosum* and *Cl. Cladosporioides*' growth on PDA, in the absence (Control) and presence of kojic acid (DOPA inhibitor) or tricyclazole (DHN inhibitor), at 10 days of incubation. Values are means of three replicates. Error bars correspond to standard deviation. Within each fungus, different symbols above the bars indicate statistically different values, according to the statistical analysis performed (Fisher's LSD test, $p < 0.05$).; Figure S2. Replicate plates with *A. niger*, grown on PDA, in the absence (Control) and presence of kojic acid (DOPA inhibitor) or tricyclazole (DHN inhibitor) at 10 days of incubation.; Figure S3. MALDI-TOF spectrum of synthetic melanin (DOPA-melanin, Sigma-Aldrich); Figure S4. MALDI-TOF spectrum of melanin extract from *Aspergillus niger*.; Figure S5. MALDI-TOF spectrum of melanin extract from *Chaetomium globosum*.; Figure S6. MALDI-TOF spectrum of melanin extract from *Cladosporium cladosporioides*.; Figure S7. The most frequent peak patterns ($m/z \pm 1$) identified in MALDI-TOF spectra from melanin samples diluted in NH_4OH.; Table S1. ^{13}C Chemical shifts of L-DOPA and 1,8-DHN model compounds.

Author Contributions: Conceptualization, methodology, resources, supervision, formal analysis, and writing—review and editing, M.C.C., S.O.S., J.A.L.; software, J.A.L.; validation, data curation, and funding acquisition, M.C.C., S.O.S.; writing—original draft preparation, D.M., T.G.P.; investigation, M.C.C., S.O.S., J.A.L., D.M., T.G.P. All authors have read and agreed to the published version of the manuscript.

Conflicts of Interest: The authors declare no conflict of interest. The funders had no role in the design of the study; in the collection, analyses, or interpretation of data; in the writing of the manuscript; or in the decision to publish the results.

References

1. Area, M.C.; Cheradame, H. Paper Aging and Degradation: Recent Findings and Research Methods. *Bioresources* **2011**, *6*, 5307–5337. [CrossRef]
2. Caneva, G.; Maggi, O.; Nugari, M.P.; Pietrini, A.M.; Piervittori, R.; Ricci, S.; Roc-cardi, A. The Biological Aerosol as a Factor of Biodeterioration. In *Cultural Heritage and Aerobiology—Methods and Measurement Techniques for Biodeterioration Monitoring*; Mandrioli, P., Caneva, G., Sabbioni, C., Eds.; Kluwer Academic Publishers: Dordrecht, The Netherlands, 2003; pp. 3–29.
3. Zotti, M.; Ferroni, A.; Calvini, P. Inhibition Properties of Simple Fungistatic Compounds on Fungi Isolated from Foxing Spots. *Restaurator* **2007**, *28*, 201–217. [CrossRef]
4. Sequeira, S.O.; Cabrita, E.J.; Macedo, M.F. Fungal Biodeterioration of Paper: How Are Paper and Book Conservators Dealing with It ? An International Survey. *Restaurator* **2014**, *35*, 181–199. [CrossRef]
5. Melo, D.; Sequeira, S.O.; Lopes, J.A.; Macedo, M.F. Stains versus Colourants Produced by Fungi Colonising Paper Cultural Heritage: A Review. *J. Cult. Herit.* **2019**, *35*, 161–182. [CrossRef]
6. Nitiu, D.S.; Mallo, A.C.; Saparrat, M.C.N. Fungal Melanins That Deteriorate Paper Cultural Heritage: An Overview. *Mycologia* **2020**, *112*, 859–870. [CrossRef]
7. Barrulas, R.V.; Nunes, A.D.; Sequeira, S.O.; Casimiro, M.H.; Corvo, M.C. Cleaning Fungal Stains on Paper with Hydrogels: The Effect of PH Control. *Int. Biodeterior Biodegrad.* **2020**, *152*, 104996. [CrossRef]

8. Gao, J.; Wenderoth, M.; Doppler, M.; Schuhmacher, R.; Marko, D.; Fischer, R. Fungal Melanin Biosynthesis Pathway as Source for Fungal Toxins. *mBio* **2022**, *13*, e0021922. [CrossRef]

9. Xu, X.; Cao, R.; Li, K.; Wan, Q.; Wu, G.; Lin, Y.; Huang, T.; Wen, G. The Protective Role and Mechanism of Melanin for Aspergillus Niger and Aspergillus Flavus against Chlorine-Based Disinfectants. *Water Res.* **2022**, *223*, 119039. [CrossRef]

10. Cordero, R.J.B.; Casadevall, A. Functions of Fungal Melanin beyond Virulence. *Fungal Biol. Rev.* **2017**, *31*, 99–112. [CrossRef]

11. Chang, P.K.; Scharfenstein, L.L.; Mack, B.; Wei, Q.; Gilbert, M.; Lebar, M.; Cary, J.W. Identification of a Copper-Transporting ATPase Involved in Biosynthesis of A. Flavus Conidial Pigment. *Appl. Microbiol. Biotechnol.* **2019**, *103*, 4889–4897. [CrossRef]

12. Eisenman, H.C.; Casadevall, A. Synthesis and Assembly of Fungal Melanin. *Appl. Microbiol. Biotechnol.* **2012**, *93*, 931–940. [CrossRef] [PubMed]

13. Tian, S.; Garcia-Rivera, J.; Yan, B.; Casadevall, A.; Stark, R.E. Unlocking the Molecular Structure of Fungal Melanin Using ^{13}C Biosynthetic Labeling and Solid-State NMR. *Society* **2003**, *42*, 8105–8109. [CrossRef] [PubMed]

14. Pinheiro, A.C.; Sequeira, S.O.; Macedo, M.F. Fungi in Archives, Libraries and Museums: A Review on Paper Conservation and Human Health. *Crit. Rev. Microbiol.* **2019**, *45*, 686–700. [CrossRef] [PubMed]

15. Trovão, J.; Mesquita, N.; Paiva, D.S.; Paiva de Carvalho, H.; Avelar, L.; Portugal, A. Can Arthropods Act as Vectors of Fungal Dispersion in Heritage Collections? A Case Study on the Archive of the University of Coimbra, Portugal. *Int. Biodeterior Biodegrad.* **2013**, *79*, 49–55. [CrossRef]

16. Sequeira, S.O.; De Carvalho, H.P.; Mesquita, N.; Portugal, A.; Macedo, M.F. Fungal Stains on Paper: Is What You See What You Get? *Conserv. Patrim.* **2019**, *32*, 18–27. [CrossRef]

17. Pal, A.K.; Gajjar, D.U.; Vasavada, A.R. DOPA and DHN Pathway Orchestrate Melanin Synthesis in Aspergillus Species. *Med. Mycol.* **2014**, *52*, 10–18.

18. Sequeira, S.O.; Laia, C.A.T.; Phillips, A.J.L.; Cabrita, E.J.; Macedo, M.F. Clotrimazole and Calcium Hydroxide Nanoparticles: A Low Toxicity Antifungal Alternative for Paper Conservation. *J. Cult. Herit.* **2017**, *24*, 45–52. [CrossRef]

19. Beltrán-García, M.J.; Prado, F.M.; Oliveira, M.S.; Ortiz-Mendoza, D.; Scalfo, A.C.; Pessoa, A.; Medeiros, M.H.G.; White, J.F.; Di Mascio, P. Singlet Molecular Oxygen Generation by Light-Activated DHN-Melanin of the Fungal Pathogen Mycosphaerella Fijiensis in Black Sigatoka Disease of Bananas. *PLoS ONE* **2014**, *9*, e91616. [CrossRef]

20. Zhang, J.; Gonzalez, E.; Hestilow, T.; Haskins, W.; Huang, Y. Review of Peak Detection Algorithms in Liquid-Chromatography-Mass Spectrometry. *Curr. Genomics.* **2009**, *10*, 388–401. [CrossRef]

21. Scigelova, M.; Hornshaw, M.; Giannakopulos, A.; Makarov, A. Fourier Transform Mass Spectrometry. *Mol. Cell. Proteom.* **2011**, *10*, M111.009431. [CrossRef]

22. Llorente, C.; Bárcena, A.; Vera Bahima, J.; Saparrat, M.C.N.; Arambarri, A.M.; Rozas, M.F.; Mirífico, M.V.; Balatti, P.A. Cladosporium Cladosporioides LPSC 1088 Produces the 1,8-Dihydroxynaphthalene-Melanin-Like Compound and Carries a Putative Pks Gene. *Mycopathologia* **2012**, *174*, 397–408. [CrossRef] [PubMed]

23. Cárdenas, G.; Cabrera, G.; Taboada, E.; Miranda, S.P. Chitin Characterization by SEM, FTIR, XRD, and ^{13}C Cross Polarization/Mass Angle Spinning NMR. *J. Appl. Polym. Sci.* **2004**, *93*, 1876–1885. [CrossRef]

24. Kumirska, J.; Czerwicka, M.; Kaczyński, Z.; Bychowska, A.; Brzozowski, K.; Thöming, J.; Stepnowski, P. Application of Spectroscopic Methods for Structural Analysis of Chitin and Chitosan. *Mar. Drugs* **2010**, *8*, 1567–1636. [CrossRef] [PubMed]

25. Šandula, J.; Kogan, G.; Kačuráková, M.; MacHová, E. Microbial (1→3)-β-D-Glucans, Their Preparation, Physico-Chemical Characterization and Immunomodulatory Activity. *Carbohydr. Polym.* **1999**, *38*, 247–253. [CrossRef]

26. Pralea, I.E.; Moldovan, R.C.; Petrache, A.M.; Ilieș, M.; Hegheș, S.C.; Ielciu, I.; Nicoară, R.; Moldovan, M.; Ene, M.; Radu, M.; et al. From Extraction to Advanced Analytical Methods: The Challenges of Melanin Analysis. *Int. J. Mol. Sci.* **2019**, *20*, 3943. [CrossRef] [PubMed]

27. Wang, L.F.; Rhim, J.W. Isolation and Characterization of Melanin from Black Garlic and Sepia Ink. *LWT* **2019**, *99*, 17–23. [CrossRef]

28. Tavzes, C.; Palcic, J.; Fackler, K.; Pohleven, F.; Koestler, R.J. Biomimetic System for Removal of Fungal Melanin Staining on Paper. *Int. Biodeterior Biodegrad.* **2013**, *84*, 307–313. [CrossRef]

29. El-Naggar, N.E.-A.; El-Ewasy, S.M. Bioproduction, Characterization, Anticancer and Antioxidant Activities of Extracellular Melanin Pigment Produced by Newly Isolated Microbial Cell Factories Streptomyces Glaucescens NEAE-H. *Sci. Rep.* **2017**, *7*, 42129. [CrossRef]

30. Gonçalves, R.C.R.; Lisboa, H.C.F.; Pombeiro-Sponchiado, S.R. Characterization of Melanin Pigment Produced by Aspergillus Nidulans. *World J. Microbiol. Biotechnol.* **2012**, *28*, 1467–1474. [CrossRef]

31. Seelam, S.D.; Agsar, D.; Halmuthur, M.S.K.; Reddy Shetty, P.; Vemireddy, S.; Reddy, K.M.; Umesh, M.K.; Rajitha, C.H. Characterization and Photoprotective Potentiality of Lime Dwelling Pseudomonas Mediated Melanin as Sunscreen Agent against UV-B Radiations. *J. Photochem. Photobiol. B* **2021**, *216*, 112126. [CrossRef]

32. Choque, E.; El Rayess, Y.; Raynal, J.; Mathieu, F. Fungal Naphtho-γ-Pyrones—Secondary Metabolites of Industrial Interest. *Appl. Microbiol. Biotechnol.* **2015**, *99*, 1081–1096. [CrossRef] [PubMed]

33. Jørgensen, T.R.; Park, J.; Arentshorst, M.; van Welzen, A.M.; Lamers, G.; vanKuyk, P.A.; Damveld, R.A.; van den Hondel, C.A.M.; Nielsen, K.F.; Frisvad, J.C.; et al. The Molecular and Genetic Basis of Conidial Pigmentation in Aspergillus Niger. *Fungal Genet. Biol.* **2011**, *48*, 544–553. [CrossRef] [PubMed]

34. Ray, A.C.; Eakin, R.E. Studies on the Biosynthesis of Aspergillin by Aspergillus Niger. *Appl. Microbiol.* **1975**, *30*, 909–915. [CrossRef] [PubMed]

35. Centeno, S.A.; Shamir, J. Surface Enhanced Raman Scattering (SERS) and FTIR Characterization of the Sepia Melanin Pigment Used in Works of Art. *J. Mol. Struct.* **2008**, *873*, 149–159. [CrossRef]

36. Culka, A.; Jehlička, J.; Ascaso, C.; Artieda, O.; Casero, C.M.; Wierzchos, J. Raman Microspectrometric Study of Pigments in Melanized Fungi from the Hyperarid Atacama Desert Gypsum Crust. *J. Raman Spectrosc.* **2017**, *48*, 1487–1493. [CrossRef]

37. Huang, Z.; Lui, H.; Chen, X.K.; Alajlan, A.; McLean, D.I.; Zeng, H. Raman Spectroscopy of in Vivo Cutaneous Melanin. *J. Biomed. Opt.* **2004**, *9*, 1198–1205. [CrossRef]

38. Martin-Sanchez, P.M.; Sanchez-Cortes, S.; Lopez-Tobar, E.; Jurado, V.; Bastian, F.; Alabouvette, C.; Saiz-Jimenez, C. The Nature of Black Stains in Lascaux Cave, France, as Revealed by Surface-Enhanced Raman Spectroscopy. *J. Raman Spectrosc.* **2012**, *43*, 464–467. [CrossRef]

39. Agarwal, U.P.; Reiner, R.S. Near-IR Surface-Enhanced Raman Spectrum of Lignin. *J. Raman Spectrosc.* **2009**, *40*, 1527–1534. [CrossRef]

40. MERCK. Melanin. Available online: https://www.sigmaaldrich.com/PT/en/product/sigma/m8631 (accessed on 11 January 2022).

41. Adhyaru, B.; Akhmedov, N.; Katritzky, A.; Bowers, C. Solid-State Cross-Polarization Magic Angle Spinning 13C and 15N NMR Characterization of Sepia Melanin, Sepia Melanin Free Acid and Human Hair Melanin in Comparison with Several Model Compounds. *Magn. Reson. Chem.* **2003**, *41*, 466–474. [CrossRef]

42. Dreyer, D.R.; Miller, D.J.; Freeman, B.D.; Paul, D.R.; Bielawski, C.W. Elucidating the Structure of Poly(Dopamine). *Langmuir* **2012**, *28*, 6428–6435. [CrossRef]

43. Hu, Y.; Hao, X.R.; Lou, J.; Zhang, P.; Pan, J.; Zhu, X.D. A PKS Gene, Pks-1, Is Involved in Chaetoglobosin Biosynthesis, Pigmentation and Sporulation in Chaetomium Globosum. *Sci. China Life Sci.* **2012**, *55*, 1100–1108. [CrossRef] [PubMed]

44. Sankawa, U.; Shimada, H.; Sato, T.; Kinoshita, T.; Yamasaki, K. Biosynthesis of Scytalone. *Tetrahedron Lett.* **1977**, *18*, 483–486. [CrossRef]

45. Yang, Y.; Lowry, M.; Xu, X.; Escobedo, J.O.; Sibrian-Vazquez, M.; Wong, L.; Schowalter, C.M.; Jensen, T.J.; Fronczek, F.R.; Warner, I.M.; et al. Seminaphthofluorones Are a Family of Water-Soluble, Low Molecular Weight, NIR-Emitting Fluorophores. *Proc. Natl. Acad. Sci. USA* **2008**, *105*, 8829–8834. [CrossRef]

46. Snyder, S.A.; Tang, Z.-Y.; Gupta, R. Enantioselective Total Synthesis of (?)-Napyradiomycin A1 via Asymmetric Chlorination of an Isolated Olefin. *J. Am. Chem. Soc.* **2009**, *131*, 5744–5745. [CrossRef] [PubMed]

47. Conradt, D.; Schätzle, M.A.; Husain, S.M.; Müller, M. Diversity in Reduction with Short-Chain Dehydrogenases: Tetrahydroxynaphthalene Reductase, Trihydroxynaphthalene Reductase, and Glucose Dehydrogenase. *ChemCatChem* **2015**, *7*, 3116–3120. [CrossRef]

48. de Oliveira, K.T.; Miller, L.Z.; McQuade, D.T. Exploiting Photooxygenations Mediated by Porphyrinoid Photocatalysts under Continuous Flow Conditions. *RSC Adv.* **2016**, *6*, 12717–12725. [CrossRef]

49. Korytowski, W.; Sarna, T. Bleaching of Melanin Pigments. Role of Copper Ions and Hydrogen Peroxide in Autooxidation and Photooxidation of Synthetic Dopa-Melanin. *J. Biol. Chem.* **1990**, *265*, 12410–12416. [CrossRef]

50. Watt, A.A.R.; Bothma, J.P.; Meredith, P. The Supramolecular Structure of Melanin. *Soft Matter* **2009**, *5*, 3754. [CrossRef]

51. Olofsson, M.A.; Bylund, D. Liquid Chromatography with Electrospray Ionization and Tandem Mass Spectrometry Applied in the Quantitative Analysis of Chitin-Derived Glucosamine for a Rapid Estimation of Fungal Biomass in Soil. *Int. J. Anal. Chem.* **2016**, *2016*, 9269357. [CrossRef]

52. Xin, C.; Ma, J.; Tan, C.; Yang, Z.; Ye, F.; Long, C.; Ye, S.; Hou, D. Preparation of Melanin from Catharsius Molossus L. and Preliminary Study on Its Chemical Structure. *J. Biosci. Bioeng.* **2015**, *119*, 446–454. [CrossRef]

53. Belozerskaya, T.A.; Gessler, N.N.; Aver'yanov, A.A. Melanin Pigments of Fungi. In *Fungal Metabolites*; Mérillo, J.-M., Ramawat, K.G., Eds.; Springer International Publishing: Berlin/Heidelberg, Germany, 2017; pp. 263–291.

54. Araújo, M.F.C. Melaninas de Origem Marinha: Caracterização Quimica e Termo-Física. Master's Thesis, Universidade de Lisboa, Lisboa, Portugal, December 2010.

55. Chang, P.K.; Cary, J.W.; Lebar, M.D. Biosynthesis of Conidial and Sclerotial Pigments in Aspergillus Species. *Appl. Microbiol. Biotechnol.* **2020**, *104*, 2277–2286. [CrossRef] [PubMed]

56. Wheeler, M.H. Comparisons of Fungal Melanin Biosynthesis in Ascomycetous, Imperfect and Basidiomycetous Fungi. *Trans. Br. Mycol. Soc.* **1983**, *81*, 29–36. [CrossRef]

57. Geib, E.; Brock, M. Comment on: "Melanisation of *Aspergillus Terreus*—Is Butyrolactone I Involved in the Regulation of Both DOPA and DHN Types of Pigments in Submerged Culture? Microorganisms **2017**, *5*, 22". *Microorganisms* **2017**, *5*, 34. [CrossRef] [PubMed]

58. Yu, R.; Liu, J.; Wang, Y.; Wang, H.; Zhang, H. Aspergillus Niger as a Secondary Metabolite Factory. *Front. Chem.* **2021**, *9*, 701022. [CrossRef] [PubMed]

59. Chiang, Y.M.; Meyer, K.M.; Praseuth, M.; Baker, S.E.; Bruno, K.S.; Wang, C.C.C. Characterization of a Polyketide Synthase in Aspergillus Niger Whose Product Is a Precursor for Both Dihydroxynaphthalene (DHN) Melanin and Naphtho-γ-Pyrone. *Fungal Genet. Biol.* **2011**, *48*, 430–437. [CrossRef]